Regular Article

Specific gene delivery to liver sinusoidal and artery endothelial cells

Tobias Abel,[1] Ebtisam El Filali,[2] Johan Waern,[3] Irene C. Schneider,[1] Qinggong Yuan,[3] Robert C. Münch,[1] Meike Hick,[4] Gregor Warnecke,[5] Nodir Madrahimov,[5] Roland E. Kontermann,[6] Jörg Schüttrumpf,[7] Ulrike C. Müller,[4] Jurgen Seppen,[2] Michael Ott,[3] and Christian J. Buchholz[1]

[1]Molecular Biotechnology and Gene Therapy, Paul-Ehrlich-Institut, Langen, Germany; [2]Tytgat Institute for Liver and Intestinal Research, Amsterdam, The Netherlands; [3]Gastroenterology, Hepatology, and Endocrinology, Hannover Medical School, and Twincore Institute for Experimental and Clinical Infection Research, Hannover, Germany; [4]Institute of Pharmacy and Molecular Biotechnology, University of Heidelberg, Heidelberg, Germany; [5]Department of Cardiac, Thoracic, Transplantation, and Vascular Surgery, Hannover Medical School, Hannover, Germany; [6]Institute of Cell Biology and Immunology, University of Stuttgart, Stuttgart, Germany; and [7]Institute for Transfusion Medicine and Immunohematology, Goethe University, Frankfurt, Germany

---

Key Points

- CD105-mediated cell entry using targeted lentiviral vectors leads to specific gene transfer of LSEC upon systemic administration.

Different types of endothelial cells (EC) fulfill distinct tasks depending on their micro-environment. ECs are therefore difficult to genetically manipulate ex vivo for functional studies or gene therapy. We assessed lentiviral vectors (LVs) targeted to the EC surface marker CD105 for in vivo gene delivery. The mouse CD105-specific vector, mCD105-LV, transduced only CD105-positive cells in primary liver cell cultures. Upon systemic injection, strong reporter gene expression was detected in liver where mCD105-LV specifically transduced liver sinusoidal ECs (LSECs) but not Kupffer cells, which were mainly transduced by nontargeted LVs. Tumor ECs were specifically targeted upon intratumoral vector injection. Delivery of the erythropoietin gene with mCD105-LV resulted in substantially increased erythropoietin and hematocrit levels. The human CD105-specific vector (huCD105-LV) transduced exclusively human LSECs in mice transplanted with human liver ECs. Interestingly, when applied at higher dose and in absence of target cells in the liver, huCD105-LV transduced ECs of a human artery transplanted into the descending mouse aorta. The data demonstrate for the first time targeted gene delivery to specialized ECs upon systemic vector administration. This strategy offers novel options to better understand the physiological functions of ECs and to treat genetic diseases such as those affecting blood factors. (*Blood*. 2013;122(12):2030-2038)

Introduction

The endothelium lining the inner surface of the vascular system performs a multitude of functions, including transport, cell migration, and cytokine secretion.[1] Depending on their respective microenvironment, endothelial cells (ECs) evolved functions focusing on specialized tasks. Of broad interest are liver sinusoidal ECs (LSEC), which are heavily fenestrated, thus promoting not only passage for a variety of substances but also uptake of particles and presentation to lymphocytes.[2,3]

As the endothelium and, especially, subtypes of ECs cannot easily be explanted and retransplanted and thus be genetically modified ex vivo, EC-specific vectors that enter only the EC type of interest after systemic administration are needed for in vivo gene transfer. Current state-of-the-art vectors for gene transfer are usually of broad tropism, ie, they enter a large variety of different cell types to express their payload. Some selectivity for ECs has been achieved by exploiting EC-specific promoters and microRNA target sequences in the transfer vector, which can detarget gene expression from particular types of non-ECs.[4,5] However, such vector particles enter into target and nontarget cells equally well, and microRNA-based detargeting cannot be used in the whole spectrum of nontarget cells.

Direct surface targeting of vectors via displayed attachment domains specific for a receptor exposed on the membrane of the EC of interest may be an option for achieving this goal. Surface targeting of lentiviral vectors (LVs) has been described before.[6-8] One system with a high, if not absolute, target cell specificity relies on engineered measles virus glycoproteins.[9] Specific targeting to a large variety of cell types such as B lymphocytes,[8] T lymphocytes,[10] dendritic cells,[11] hematopoietic progenitors,[9] neurons,[9] and tumor cells[12,13] via the corresponding cell surface marker proteins has demonstrated the unique flexibility of this vector system. Specificity is usually mediated by a single-chain variable fragment (scFv) with high affinity for the target receptor fused to the measles virus hemagglutinin envelope protein engineered to be deficient in natural receptor binding. By displaying a scFv specific for human endoglin (CD105), a targeting vector for human ECs (huCD105-LV) has been generated, which demonstrated unprecedentedly high specificity in vitro.[9]

As a cofactor in the TGF-β signaling pathway, CD105 is conserved in sequence and expression profile between human and mouse.[14,15] Here, we investigated the in vivo gene delivery mediated by systemically applied CD105-targeted vectors. A newly generated

---

mouse CD105-specific vector was highly specific and effective in genetic modification of LSECs even when applied systemically. Correspondingly, huCD105-LV specifically transduced human LSECs or vascular arterial ECs in 2 different xenograft mouse models.

Methods

Primary cells and tissue

Mouse nonparenchymal liver cells were prepared from CO_2-sacrificed, adult, C57Bl/6 mice, which were perfused through the left ventricle with 5-10 mL prewarmed liver perfusion medium (Gibco; Life Technologies, Darmstadt, Germany) for 10 minutes, followed by 5-10 mL liver digestion medium (Gibco) supplemented with collagenase IV (Serva, Heidelberg, Germany) for 5 minutes. Parenchymal cells were eliminated by centrifugation for 4 minutes at $50g$. The supernatant was pelleted at $150g$ for 5 minutes and plated in EC growth medium–2 (PromoCell, Heidelberg, Germany) supplemented with 5% fetal calf serum (FCS), 100 U/mL penicillin and 100 μg/mL streptomycin in rat-tail collagen-coated 24-well plates. Medium was changed after 6 hours, and transduction was performed on the next day. Animal experiments were performed according to the German animal protection law.

Human pulmonary arteries and human saphenous veins were obtained with approval of the local ethics committee of the Medizinische Hochschule Hannover and after written consent from patients undergoing cardiopulmonary surgery in accordance with the Declaration of Helsinki. Vessels were immediately transferred into ice-cold phosphate-buffered saline (PBS) to remove blood cells. Transduction with huCD105-LV was carried out 1-2 hours after surgery in EC growth medium (C-22010; Promocell) using 5×10^7 transducing units/dish. Medium was replaced after 24 hours and changed every 2 days. Green fluorescent protein (GFP) fluorescence was monitored 8-10 days later by immunofluorescence microscopy.

Human fetal liver cells were obtained after informed consent in accordance with the Declaration of Helsinki, and the use was approved by the Medical Ethical Committee at the Academic Medical Center of Amsterdam.

Vector production and transduction

Seven different vector types were applied in this work: LVs specific for murine CD105 transferring GFP (mCD105-LV[GFP]); luciferase (mCD105-LV[luc]); luciferase and GFP (mCD105-LV[luc-GFP]); erythropoietin (mCD105-LV[Epo]); LVs specific for human CD105 transferring luciferase and GFP (huCD105-LV[luc-GFP]); and vesicular stomatitis virus glycoprotein (VSV-G)–pseudotyped LVs transferring GFP (VSV-G-LV[GFP]), as well as luciferase and GFP (VSV-G-LV[luc-GFP]). Vectors were produced by polyethyleneimine-mediated transfection of human embryonic kidney 293T cells (CRL-11268; American Type Culture Collection, Manassas, VA) seeded 1 day before transfection (1.6×10^7 cells per T175 flask). Immediately before transfection, medium was replaced by 13 mL Dulbecco's modified Eagle medium (DMEM) containing 15% FCS and 1.5% glutamine. We mixed 1.3 μg pCG-H$_{mut}$-αmCD105 with 4.1 μg of pCG-FcΔ30,[8] 14.6 μg of pCMV-ΔR8.9[16] packaging plasmid, and 15 μg transfer vector plasmid in 2.3 mL DMEM. We diluted 140 μL of 18 mM polyethyleneimine solution into 2.2 mL DMEM. Both solutions were combined, mixed, and incubated for 20 minutes before they were added to the cells. Next day, medium was exchanged and supernatant collected 24 hours later and cleared by filtration through a 0.45-μm filter. Vector particles were then centrifuged through a 20% (weight/volume) sucrose cushion for 25 hours at $4500g$ at 4°C. Vector particles were resuspended in Opti-MEM (Gibco) and stored at −80°C in aliquots.

Transduction was performed in 24-well plates 1 day after seeding. Vector stocks were diluted into 250 μL of medium supplemented with 4 ng/mL protamine sulfate (Sigma-Aldrich, Taufkirchen, Germany). After 14 hours, 750 μL medium was added.

Animal experiments

For all in vivo targeting experiments, Athymic Nude-Foxn1[nu] mice (Harlan, Rossdorf, Germany) were injected once with 200 μL of vector stock diluted in Opti-MEM. Tumor xenografts were established by subcutaneous implantation of 5×10^6 human breast cancer–derived MCF-7 cells (HTB-22; American Type Culture Collection) into the right flank of Athymic Nude-Foxn1[nu] until they reached a volume of 200-400 mm³. For intratumoral application, 100 μL vector was injected fan-shaped through a 27-G needle. For in vivo imaging, mice were injected intraperitonially with 250 μL luciferin (150 mg/kg body weight), anesthetized with 2.5% isoflurane, and analyzed within 10 to 20 minutes after luciferin administration. Images were acquired on an Ivis Spectrum optical imager (Caliper Life Science, Hopkinton, MA) and analyzed using Living Image 4 software (PerkinElmer, Waltham, MA). Aortic interposition grafts were performed with human internal mammarian artery side branches transplanted into the abdominal aorta of NOD/c.rag2^{−/−}c.γ[−/−] (NRG) mice with an end-to-end anastomosis using a technique described by Koulack et al.[17]

Human liver EC engraftment was achieved by intrasplenic injection of 1×10^6 human liver ECs in Rag2^{−/−}yc^{−/−} mice (N = 4). Mice were sacrificed and fixed by in vivo perfusion, and livers were excised for histology and immunohistochemistry as described.[18]

After erythropoietin gene transfer, hematology was performed on a Scil Vet ABCCounter (Scil Animal Care, Viernheim, Germany).

Histology and immunostaining

Mice were sacrificed by CO_2 and perfused through the left ventricle with PBS, followed by 4% formaldehyde in PBS. Livers or tumor slices were incubated in 4% formaldehyde for 4 to 6 hours before dehydration in ascending sucrose concentrations and finally snap frozen in optical cutting temperature medium (Sakura Finetek, Staufen, Germany). We permeabilized 8-9 μm cryosections for 15 minutes in 0.25% TritonX100/PBS, blocked with 10% donkey serum, and incubated with rat anti-CD31 antibody (1:20, SZ31; Dianova, Hamburg, Germany), rat anti-F4/80 (1:200, BM8; Dianova) or the GFP-specific rabbit antiserum (1:400; Life Technologies), respectively. For detection, donkey anti-rat DyLight-549 F(ab)₂ (1:250; Dianova) and donkey anti-rabbit Dylight-649 (1:250; Biolegend, San Diego, CA) were applied. Stained tissue was embedded in Fluoroshield with DAPI (Sigma-Aldrich).

Human vessels were fixed in 4% paraformaldehyde followed by 30% sucrose before embedding in Tissue-Tek (Sakura) and cryosectioning for immunofluorescence staining. Sections were probed with primary antibodies rabbit anti-GFP (1:200; Life Technologies) and mouse anti-huCD105-APC (1:3; Miltenyi Biotec, Bergisch Gladbach, Germany) and appropriate secondary antibodies. Immunofluorescence was acquired at an Olympus IX81 immunofluorescence microscope using Cell-M software (Olympus, Hamburg, Germany).

Statistical analysis

All data are displayed as mean and the standard error of the mean. Statistical significance between 2 groups was determined using unpaired Student t tests. P values are given in the figure legends. A P value of less than .05 was considered significant.

Results

Targeting gene transfer to murine CD105

To generate a LV specific for mouse ECs, we displayed the scFv mE12, which binds mouse but not human CD105 with nanomolar affinity[19] on the H protein (see supplemental Data found on the *Blood* Website for details). The H$_{mut}$-mE12 fusion protein was readily expressed on the cell surface and efficiently incorporated into LV particles along with the F protein (supplemental Figure 1). HT1080 cells stably expressing mouse CD105 were efficiently transduced by mCD105-LV while even at a high vector dose, no GFP expression on the parental, murine CD105-negative, HT1080 cells
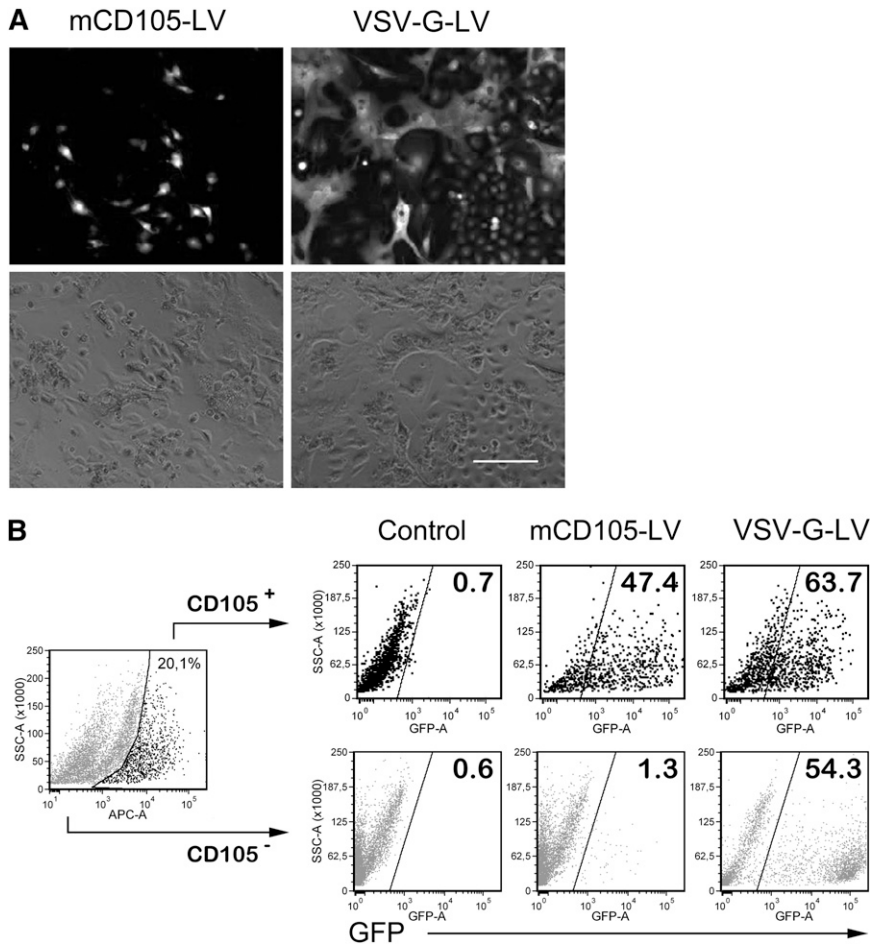
Figure 1. Transduction of primary liver cells. Mouse nonparenchymal liver cells were isolated and cultivated for 36 hours before mCD105-LV or VSV-G-LV were added (multiplicity of infection of 3, respectively). (A) After 96 hours, photographs were taken under fluorescence (top) and bright field microscopy (bottom). Scale bar: 200 μm. (B) Cells were then detached to quantify the percentage of GFP-positive cells in the CD105-positive fraction (upper panel) and CD105-negative fraction (bottom panel) by flow cytometry using rat anti-mouse CD105-APC (1:20, MJ7/18; Miltenyi Biotec). Data were acquired on a LSRII- fluorescence-activated cell sorter (BD Bioscience, Heidelberg, Germany) and analyzed using the FCS-express software (Denovo Software, Los Angeles, CA).

was observed (supplemental Figure 2A). Likewise, mCD105-LV transduced up to 50% of primary endothelial endoglin positive cells without interfering with their ability to form capillarylike structures (supplemental Figure 2B-C).

Together with Kupffer cells, LSECs comprise about 30% of all liver cells. Because it is well established that VSV-G-LV is taken up by Kupffer cells,[20,21] mCD105-LV was next tested on cultures of nonparenchymal primary liver cells consisting mostly of LSECs and Kupffer cells and less than 10% hepatocytes. Upon incubation with mCD105-LV, only distinct polygonally shaped cells in the size of LSECs[22] became GFP-positive, whereas cells with a great variability in morphology were transduced with VSV-G-LV (Figure 1A). These observations were confirmed by flow cytometry (Figure 1B). While VSV-G-LV transduced CD105-positive and -negative cells equally well, almost 50% of the CD105-positive cells had become GFP-positive upon mCD105-LV treatment in comparison with less than 1.5% GFP-positive cells in the CD105-negative fraction.

Systemic in vivo gene transfer

Next we analyzed gene transfer mediated by mCD105-LV in vivo upon systemic administration. Transduced cells were tracked by in vivo imaging (via the transferred luciferase gene) and by histology (via the transferred GFP gene). The by far strongest luciferase activity (73.6 ± 10%; N = 6) in the mCD105-LV group was present in liver (Figure 2A). VSV-G-LV showed strong signals in liver, too (50.5 ± 15.2%; N = 6), but gave in addition rise to signals

in bone (26.9 ± 8.6%) and spleen (6.4 ± 4.4%). This pattern of transgene expression was maintained over the whole observation period of more than 4 weeks. The strong preference of mCD105-LV for liver gene transfer was further confirmed by determining the luciferase activities in organ lysates. Over a range of 3 different vector doses, more than 90% of the activity was detected in liver. Spleen exhibited the second strongest activity, and negligible activities were present in lung, heart, kidney, brain, and lymph nodes (supplemental Figure 4).

In histology, Kupffer cells were identified by the specific marker F4/80 and liver ECs via CD31, because available antibodies against mouse CD105 are nonfunctional in formaldehyde-fixed tissue, which is essential for proper GFP detection.[23] GFP signals in the mCD105-LV-treated group did not colocalize with the strong CD31 staining of large blood vessels (Figure 2B, left panel) but were restricted to a population of cells exhibiting the typical morphology of LSECs (thin cells, lining the capillary sinuses of the liver) (supplemental Figure 3). LSECs express only low levels of CD31,[24] and costaining for CD31 and GFP was detected at high magnification (Figure 2B, right panel). There was no evidence for GFP expression by stellate cells, which have been found to be CD105-positive.[25] While in the VSV-G-LV-injected mice, about 85% of the GFP-positive cells colocalized with the Kupffer cell–specific F4/80 antigen; only a few GFP-positive cells were F4/80-positive in the mCD105-LV-injected group (Figure 2C).[26] In the mCD105-LV group, 98% of all GFP-positive cells also expressed CD31, and in the VSV-G-LV group, only 14% (Figure 2D).
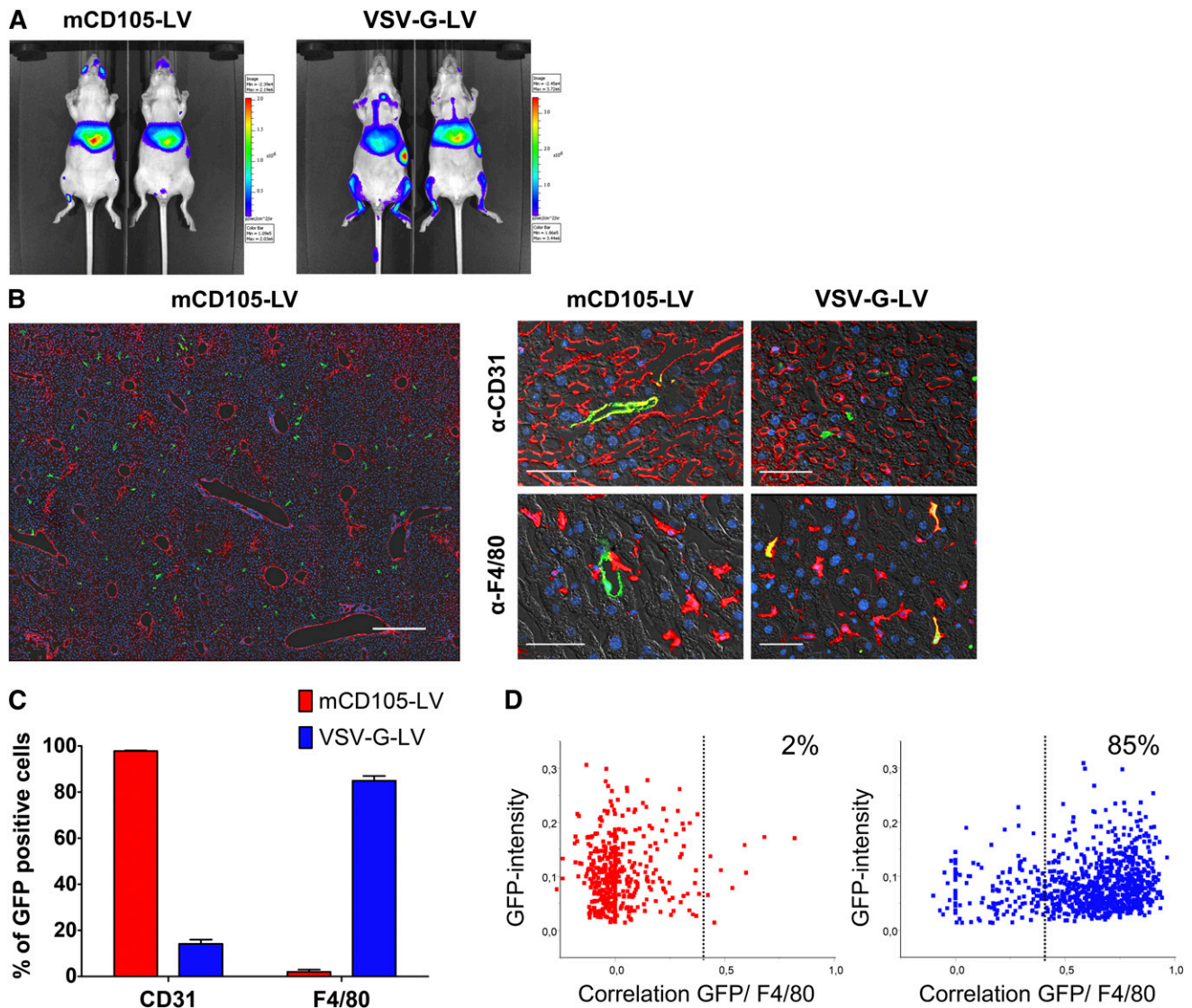
Figure 2. Reporter gene expression of systemically applied mCD105-LV. Mice were injected intravenously in the tail vein with mCD105-LV or VSV-G-LV (single dose of 2×10^6 transducing units, respectively), transferring a bicistronic luciferase-GFP reporter gene (pS-luc2-GFP-W). (A) In vivo luminescence imaging monitored 2 weeks after vector injection. Two representative mice out of 6 are shown for each group. (B) Mice were sacrificed at 2 weeks after vector injection, and livers were excised for histology. Images were acquired on a fully automated Axio-Observer Z1 microscope equipped with an ApoTome optical sectioning unit (Carl Zeiss, Jena, Germany). For quantification, 4 large high-resolution images from different liver areas were assembled by acquisition of 100 adjacent fields of view per section at 20× magnification using the MosaiX module (Carl Zeiss). The left panel shows a representative overview of mCD105-LV transduced mouse liver comprising 100 tiles at 20× magnification stained against CD31 (red), GFP (green), and with 4,6 diamidino-2-phenylindole (DAPI) (blue). Scale bar: 500 μm. The right panel shows a higher magnification of representative sections stained either against CD31 for LSEC (upper right) or against F4/80 for Kupffer cells (lower right). Scale bar: 25 μm. (C) Quantification of GFP colocalization with F4/80 or CD31, respectively, for mCD105-LV (red) and VSV-G-LV (blue) injected mice. Per marker and vector, 4 sections derived from 2 mice, corresponding to a total liver area of 62 mm², in total more than 100 000 cells corresponding to about 500 transduction events, were analyzed. Morphometric analysis for F4/80/GFP-colocalization as well as nuclei quantification was performed using the Cell Profiler software.[26] CD31/GFP colocalization was quantified by manual counting. (D) Results from morphometric analysis of Kupffer cell transduction. Intensities of GFP-positive cells were correlated to F4/80 staining and plotted against the total GFP intensity of the respective cells. Below the threshold of 0.35, no Kupffer cell transduction was observed.

Targeting tumor ECs

Next, we assessed the transduction of ECs in mice carrying a vascularized human tumor xenograft growing subcutaneously. We selected the MCF-7 tumor model, which is known to induce CD105-positive neovasculature originating from the host's tissue.[27] When mCD105-LV[luc] was injected intratumorally, luciferase activity was restricted to the tumor (Figure 3A). Several consecutive tumor tissue slices were luciferase-positive. Histology revealed that all cells transduced by the vector exhibited the typical morphology of ECs but not that of tumor cells. CD31, which is known to be expressed in later stage of tumor angiogenesis than is CD105,[28] was detected on

many of these cells (Figure 3B). ECs in tumor tissue were also transduced upon systemic administration of mCD105-LV but to a much lower extent (Figure 3A). In this setting, the vast majority of luciferase activity was present in liver (Figure 3A).

Delivery of the erythropoietin gene by mCD105-LV

Next, we analyzed whether the LSEC-restricted gene transfer mediated by mCD105-LV allows delivery of biologically active erythropoietin into immunodeficient and -competent mice.[29] In vitro, mCD105-LV[Epo] mediated efficient erythropoietin expression in a dose-dependent manner in target cells (supplemental
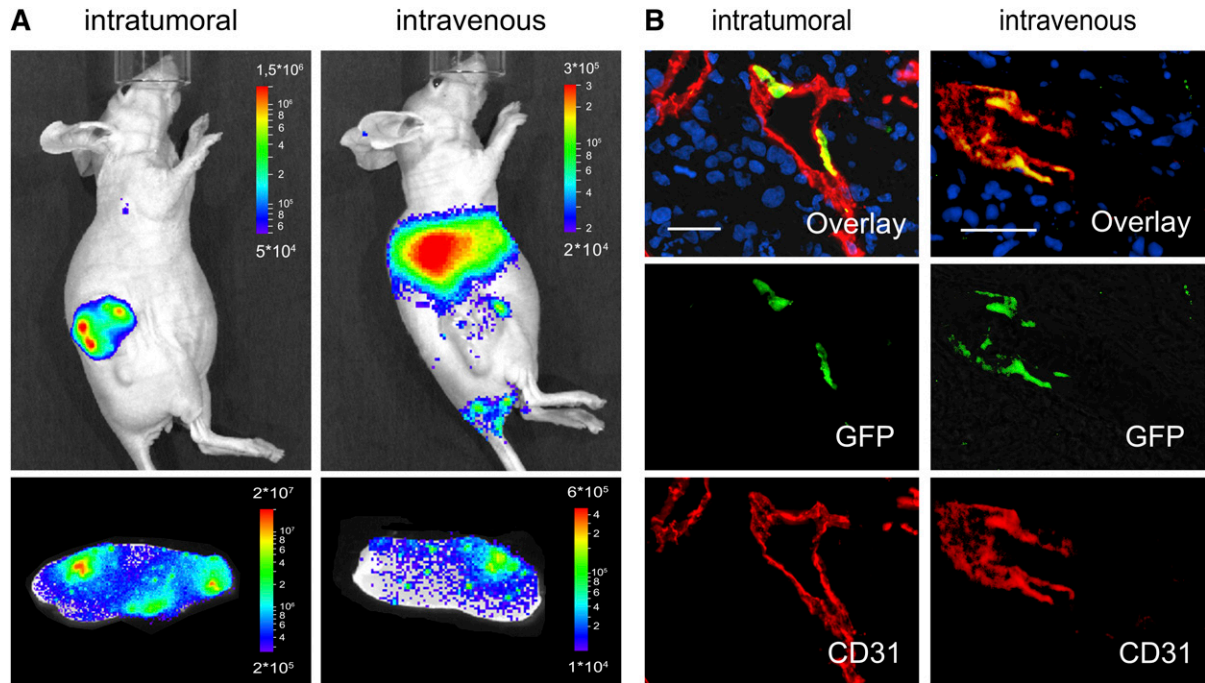
Figure 3. Targeting tumor ECs. Athymic nude mice bearing subcutaneous MCF-7 tumors were injected with either 1×10^6 transducing units intratumorally or 2×10^6 transducing units intravenously with mCD105-LV transferring luciferase (A) or GFP (B). Gene transfer was analyzed 5 days after vector injection by luciferase imaging (A) and histology (B). (A) Luciferase imaging of the whole living animal (upper panel) or in dissected tumor slices (~2 mm in width, lower panel). (B) On the cellular level, gene transfer was visualized by immunofluorescence of explanted tumors with antibodies specific for mouse CD31 (red, lower panel), GFP (green, center panel), and merge (upper panel). Nuclei in the 9-μm cryosections were stained by DAPI (blue). Scale bar, 30 μm.

Figure 6). In injected nonobese diabetic (NOD)–severe combined immunodeficiency (SCID) mice, erythropoietin levels increased to above eightfold of baseline by day 4 and to more than 25-fold of
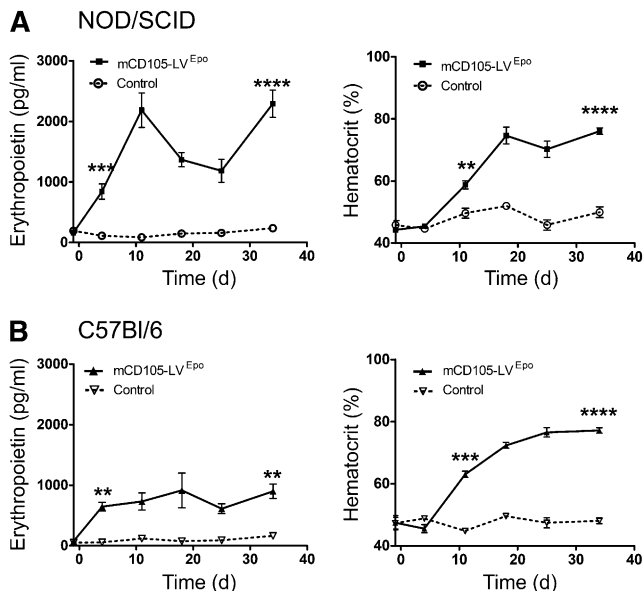

Figure 4. Erythropoietin gene transfer by mCD105-LV. (A) Immunodeficient NOD/SCID mice (N = 5) or (B) immunocompetent C57Bl/6 mice (N = 3) were injected once intravenously with 3×10^6 transducing units mCD105-LV^{Epo} (solid symbols) or medium (open symbols, dotted lines) on day 0. Two days before tail-vein injection, blood samples were taken and hematological baseline levels were determined. Erythropoietin levels in blood (left panel) as well as hematocrit values (right panel) were determined regularly at the indicated time points. **$P < .01$; ***$P < .001$; ****$P < .0001$, as determined by unpaired 2-sided t tests.

the physiological level by the end of the observation period (Figure 4A). The hematocrit followed the erythropoietin levels with a delay of 3-5 days, finally reaching almost 80%. In all treated animals, spleen size had increased by more than fourfold (supplemental Figure 7), further confirming the high red blood cell load. In C57Bl/6 mice, mCD105-LV^{Epo} raised erythropoietin levels by about 10-fold, resulting in a similar high hematocrit value as in NOD/SCID mice, indicating that CD105 targeting did not induce an immune response against transduced cells (Figure 4B).

In vivo targeting of human CD105-positive cells

We next studied huCD105-LV[9] in vivo. Stocks of this vector were on average threefold more potent in titer than those of its murine counterpart mCD105-LV. For this purpose, Rag2$^{-/-}$yc$^{-/-}$ mice were reconstituted with human liver ECs, resulting in patches of humanized liver endothelium as described previously.[18] Only CD31-positive cells exhibiting the typical morphology of ECs were transduced by huCD105-LV (Figure 5A). No murine LSECs or F4/80-positive Kupffer cells were transduced, demonstrating the cell specificity of huCD105-LV (Figure 5A). The majority of LSEC clusters were at least partially transduced, whereas just about 15% showed no GFP expression (Figure 5B). On average, approximately 40% of the human LSEC showed GFP expression. In control mice without human LSECs, no transduction was detected (supplemental Figure 8). Thus, even in the absence of target cells, no off-target gene transfer occurred.

We next asked whether huCD105-LV can also transduce ECs present in larger blood vessels. A small part of a human saphenous vein, explanted after coronary bypass surgery, was incubated with huCD105-LV ex vivo. GFP expression was detected exclusively in CD105-positive cells lining the vessel lumen (Figure 6A). Efficient

Figure 5. Transduction of human liver EC repopulated mice by huCD105-LV. Rag2$^{-/-}$yc$^{-/-}$ mice were repopulated with human liver ECs. Two weeks after reconstitution, mice were injected once with 2×10^6 transducing units huCD105-LV. (A) Six to 8 days after vector injection, liver sections were stained for human CD31 (upper panel) or F4/80 (lower panel). Nuclei were stained with DAPI. GFP expression was observed by direct fluorescence. GFP/CD31 double-positive clusters of repopulated human liver ECs are indicated by arrows. Scale bars: 29.63 μm (upper panel) and 27.12 μm (lower panel). No GFP positive cells were detected after administration of huCD105-LV to mice without human liver endothelium (supplemental Figure 8). (B) Because individual human LSECs cannot be identified within the tightly connected clusters in the mouse liver, the amount of GFP-positive cells in the CD31-positive clusters was divided in quintiles of 0%, 25%, 50%, 75%, or 100% GFP expression. The relative quantities of these quintiles are plotted.
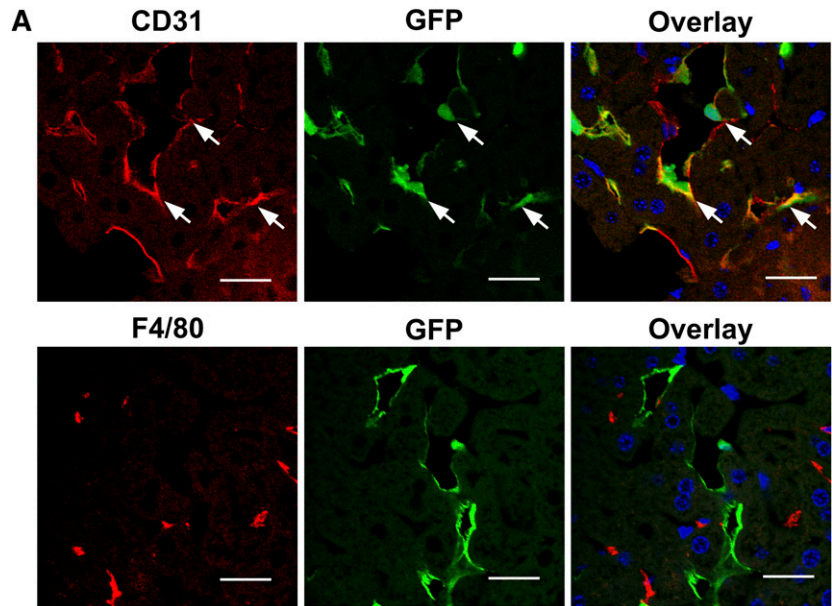
EC transduction was also observed in a human artery in a similar setup (supplemental Figure 9). Next, arteries were transplanted intra-abdominally into the descending aorta of recipient mice. Systemically applied huCD105-LV precisely transduced CD105-positive cells lining the inner lumen of the xenograft (Figure 6B). No GFP signals were detectable in sections of the inferior vena cava, heart, spleen, or liver (data not shown).

Discussion

We demonstrate that specialized ECs can be specifically targeted to express reporter or therapeutic genes upon systemic administration of rationally designed LVs. The targeting strategy relies on the specificity of the scFv displayed on the vector surface, in this case directed against CD105 (endoglin). It was surprising that both the murine and human CD105-targeted vectors were so efficient and specific for LSECs when injected intravenously into the tail vein of mice. A single-vector injection was sufficient to reach 8×10^5 LSECs per liver, which corresponds to about 40% of the administered vector particles having transduced LSECs. This number is supported by more than 90% of the overall luciferase activity found to be present in liver. Thus, a high fraction of the administered vector particles must have hit LSECs. In contrast, conventional LVs pseudotyped with VSV-G show a clear preference for Kupffer cells. Only at a high dose

can other liver cells—including hepatocytes, LSECs, and stellate cells—also be hit.[30-32]

To end up in LSECs after tail vein injection, the targeted vector particles must have bypassed the endothelium of the vena cava, lung, and heart. Expression profiles for murine CD105 are based on polymerase chain reaction or histology. The bottom line from these publications is that CD105 is predominantly expressed on cells of the microvascular endothelium and ECs present in tissue undergoing active angiogenesis, eg, during regeneration or tumor vascularization.[33] In healthy, adult animals, CD105 is mainly expressed in the distal arteries, distal veins, and capillaries of lung and liver.[22,28,34]

The pronounced preference of mCD105-LV particles for liver LSECs is most likely due to a combination of vector particle properties, blood circulation kinetics, and accessibility of the CD105 receptor for the vector particles present in the lumen of the blood vessels. We know from previous work with huCD105-LV,[9] but also other targeting vectors,[12] that transduction efficiency closely correlates with the cell surface density of the targeted receptor. It is also therefore likely that mCD105-LV preferentially transduces those cells displaying the highest CD105 density. Quantitative data for the CD105 densities on CD105-positive cells are not available. However, at least for stellate cells, which have been defined as CD105-positive by biochemical data,[25] the CD105 density must be much lower than that on LSECs, because these can be easily purified from liver using CD105-specific antibodies.[22] In addition, stellate cells are rather inaccessible for systemically applied mCD105-LV because these
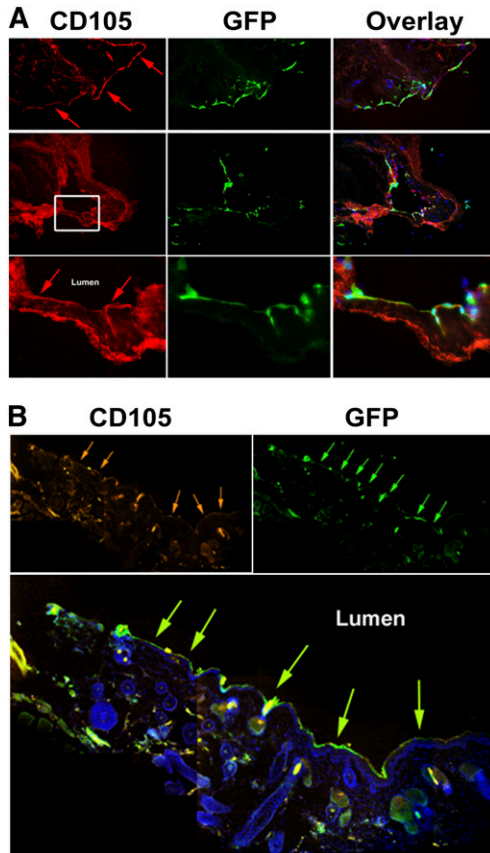
Figure 6. Ex vivo and in vivo transduction of human vessels. (A) Human saphenous veins were removed from patients undergoing coronary bypass surgery and transferred immediately into culture dishes. The vessels were transduced with huCD105-LV and cultivated for 7-10 days before fixation and immunofluorescent staining. Cells were stained for human CD105 (left column) or for GFP (middle column), or were merged to display colocalization (right column). Arrows point to the luminal side of the vessel. (B) Mammarian arteries from patients requiring coronary bypass surgery were transplanted intraabdominally into the descending aorta of NOD Rag2$^{-/-}$IL-2Rγc^{null} mice. HuCD105-LV (3×10^7 transducing units) was injected into the tail vein of transplanted mice at 2, 5, and 8 days after transplantation, and mice were sacrificed after 16 days. The transplanted artery was cryosectioned and prepared for immunofluorescence staining. The pictures were acquired by detecting fluorescence at 4 adjacent locations along the luminal endothelial layer of the transduced graft. Raw picture data were obtained by acquiring fluorescence in the GFP, the DAPI, and the Cy5 channel. The channels were merged using the Olympus Cell^M image acquiring and processing software. To obtain an overview of the entire stretch of the transduced endothelium, we assembled 4 pictures using Adobe Photoshop software (Adobe Systems, San Jose, CA). Hangover areas were filled with black color to generate a high-contrast background. Noise was reduced by balancing color levels equally for assembled pictures. The staining revealed CD105-positive cells lined up facing the lumen (orange arrows, top left), which were also positive for GFP (green arrows, top right). Colocalization is depicted in the merge (bottom, green arrows). Representative pictures are from 1 mouse, 3 mice transplanted.

would have to pass the endothelium to reach the space of Disse.[35] Resting vascular ECs express only low levels of CD105 and, moreover, the velocity of blood flow is relatively high in large vessels, but slows down substantially in the sinuses of the liver.[3,18] At low flow rates the likelihood for functional contacts between CD105-LV and CD105 leading to gene delivery is considerably enhanced. This explains the efficient gene delivery observed for mCD105-LV and for huCD105-LV in EC-transplanted mice. We did, however, also observe gene transfer into ECs exposed to high blood flow, ie, into transplanted arteries, upon systemic administration of huCD105-LV. Although this clearly demonstrates the potency of vector targeting, it has to be considered that this was

achieved at an approximately 30-fold–higher vector dose administered by multiple vector applications. Moreover, as by this approach a human receptor was targeted in a mouse environment, vector particles could most likely travel several rounds through the circulation until they reached their target cells in the transplanted artery.

Our data thus demonstrate that EC targeting in vivo is not only determined by the specificity of the targeting domain displayed on the vector surface but can be controlled through the application route and the presence and accessibility of target cells. This is nicely illustrated in the tumor model we investigated. Although local intratumoral injection resulted in gene transfer to the tumor ECs and absence of LSEC gene transfer, tail vein vector injection resulted in the opposite: most of the gene transfer activity in liver and only minor activity in tumor ECs. This biodistribution of mCD105-LV corresponds well to that of CD105-specific antibodies systemically applied into tumor-bearing mice. Such antibodies end up mainly in liver and spleen, and only a minority labels the tumor vasculature.[36,37]

The data provided here for a systemically applied vector recognizing a mouse receptor in the mouse environment places the measles virus glycoprotein–based targeting system in a unique position among other vector systems. For LV, the alternative targeting technology based on engineered Sindbis virus envelope proteins[38] has only been evaluated ex vivo for EC targeting (via transferrin receptor or via CD146) but not in vivo.[39,40] Besides LV, AAV vectors have been redirected to ECs by displaying small endothelium-specific peptides on their capsid.[41] However, transduction of liver as nontarget tissue was only moderately reduced, and off-targeting on a cellular level was not quantified,[42] suggesting that this approach with AAV vectors rather leads to an extension of vector tropism than to a complete restriction to a specialized EC type as demonstrated here for CD105 targeting.

Although the specificity of the CD105-targeted vectors is unprecedented, functional titers are at present lower than those of VSV-G-LV. Despite this, our experiments impressively demonstrate that a single tail vein injection of mCD105-LV^{Epo} was sufficient to increase erythropoietin levels in the circulation to 25-fold above physiological values. Importantly, dose-response analysis revealed no toxicity in treated animals, and liver enzyme values remained unchanged even at a particle dose (15 µg p24), similar to that which substantially raised liver transaminase levels for VSV-G-LV (25 µg p24)[43] (supplemental Figure 5). These and the resulting high hematocrit values remained constant over several weeks in immunocompetent mice also, indicating that no cellular immune response against the transduced cells was mounted. This indicates that off-target related unwanted effects typically observed for VSV-G-LVs can be avoided by targeted CD105-LVs. It remains to be seen whether functional particle titers need to be further increased for the efficient delivery of other therapeutic gene products in a clinical setting. To this end, vector production may be improved by CD105-specific affinity chromatography of particles or by replacing scFv with CD105-specific ankyrin repeat proteins that we recently demonstrated as very effective and highly stable targeting motifs.[12] The vectors described here will facilitate functional studies of specialized ECs in their natural environment. Physiological changes can now be evidently linked to the genetic modifications introduced into the EC type of choice. In different settings, LSECs promoted immunotolerance to model antigens rather than immunity.[22,43,44] Interestingly, after systemic injection of transcriptionally targeted vectors specific for either hepatocytes or LSEC, immunoreactivity against GFP was even more reduced in the hepatocyte group, demonstrating immunomodulatory functions of other liver cell populations.[5] The CD105

targeting described here will be instrumental in further clarifying the role of LSECs for the long-term expression of foreign immunogenic molecules.

In addition, the unique specificity of CD105 targeting for LSECs offers the possibility of restricting gene delivery and expression of therapeutic proteins to be released into the blood stream to cells that naturally fulfill this task. An important example here is hemophilia A, for which an efficacious gene therapy strategy is still lacking.[44] Finally, cancer (CD105 overexpression in ECs)[45] and liver fibrosis (exhibiting CD105 overexpression in hepatic stellar cells)[25] can be added to the list of potential therapeutic target diseases for CD105-specific vectors.

Authorship

Contribution: T.A. designed and performed experiments and contributed to writing of the manuscript; E.E.F, J.W., I.C.S., Q.Y., R.C.M., M.H., G.W., and N.M. performed experiments; R.E.K. contributed vital reagents; J. Schüttrumpf and U.C.M. contributed to study design; J. Seppen and M.O. contributed to supervision of work and writing of the manuscript; and C.J.B. conceived and designed the study, acquired grants, supervised work and wrote the manuscript.

Conflict-of-interest disclosure: The authors declare no competing financial interests.

Correspondence: Christian J. Buchholz, Paul-Ehrlich-Institut, Molecular Biotechnology and Gene Therapy, Paul-Ehrlich-Str. 51-59, Langen, Hessen D-63225, Germany; e-mail: christian.buchholz@pei.de.

References

1. Aird WC. Spatial and temporal dynamics of the endothelium. *J Thromb Haemost.* 2005;3(7): 1392-1406.

2. Stolz DB. Sinosoidal endothelial cells. In: Monga SPD, ed. Molecular Pathology of Liver Diseases. New York, NY: Springer; 2011:97-107.

3. Thomson AW, Knolle PA. Antigen-presenting cell function in the tolerogenic liver environment. *Nat Rev Immunol.* 2010;10(11):753-766.

4. White SJ, Nicklin SA, Büning H, et al. Targeted gene delivery to vascular tissue in vivo by tropism-modified adeno-associated virus vectors. *Circulation.* 2004;109(4):513-519.

5. Annoni A, Brown BD, Cantore A, Sergi LS, Naldini L, Roncarolo MG. In vivo delivery of a microRNA-regulated transgene induces antigen-specific regulatory T cells and promotes immunologic tolerance. *Blood.* 2009;114(25):5152-5161.

6. Morizono K, Xie Y, Ringpis GE, et al. Lentiviral vector retargeting to P-glycoprotein on metastatic melanoma through intravenous injection. *Nat Med.* 2005;11(3):346-352.

7. Yang L, Bailey L, Baltimore D, Wang P. Targeting lentiviral vectors to specific cell types in vivo. *Proc Natl Acad Sci USA.* 2006;103(31):11479-11484.

8. Funke S, Maisner A, Mühlebach MD, et al. Targeted cell entry of lentiviral vectors. *Mol Ther.* 2008;16(8):1427-1436.

9. Anliker B, Abel T, Kneissl S, et al. Specific gene transfer to neurons, endothelial cells and hematopoietic progenitors with lentiviral vectors. *Nat Methods.* 2010;7(11):929-935.

10. Zhou Q, Schneider IC, Edes I, et al. T-cell receptor gene transfer exclusively to human CD8(+) cells enhances tumor cell killing. *Blood.* 2012;120(22):4334-4342.

11. Ageichik A, Buchholz CJ, Collins MK. Lentiviral vectors targeted to MHC II are effective in immunization. *Hum Gene Ther.* 2011;22(10): 1249-1254.

12. Münch RC, Mühlebach MD, Schaser T, et al. DARPins: an efficient targeting domain for lentiviral vectors. *Mol Ther.* 2011;19(4):686-693.

13. Ou W, Marino MP, Suzuki A, et al. Specific targeting of human interleukin (IL)-13 receptor α2-positive cells with lentiviral vectors displaying IL-13. *Hum Gene Ther Methods.* 2012;23(2): 137-147.

14. St-Jacques S, Cymerman U, Pece N, Letarte M. Molecular characterization and in situ localization of murine endoglin reveal that it is a transforming growth factor-beta binding protein of endothelial and stromal cells. *Endocrinology.* 1994;134(6): 2645-2657.

15. Warrington K, Hillarby MC, Li C, Letarte M, Kumar S. Functional role of CD105 in TGF-beta1 signalling in murine and human endothelial cells. *Anticancer Res.* 2005;25(3B):1851-1864.

16. Zufferey R, Nagy D, Mandel RJ, Naldini L, Trono D. Multiply attenuated lentiviral vector achieves efficient gene delivery in vivo. *Nat Biotechnol.* 1997;15(9):871-875.

17. Koulack J, McAlister VC, Giacomantonio CA, Bitter-Suermann H, MacDonald AS, Lee TD. Development of a mouse aortic transplant model of chronic rejection. *Microsurgery.* 1995;16(2): 110-113.

18. El Filali E, Hiralall JK, Veen HA, Stolz DB, Seppen J. Human liver endothelial cells, but not macrovascular or microvascular endothelial cells engraft in the mouse liver [published online ahead of print Oct. 3, 2012]. *Cell Transplant.*

19. Müller D, Trunk G, Sichelstiel A, Zettlitz KA, Quintanilla M, Kontermann RE. Murine endoglin-specific single-chain Fv fragments for the analysis of vascular targeting strategies in mice. *J Immunol Methods.* 2008;339(1):90-98.

20. van Til NP, Markusic DM, van der Rijt R, et al. Kupffer cells and not liver sinusoidal endothelial cells prevent lentiviral transduction of hepatocytes. *Mol Ther.* 2005;11(1):26-34.

21. Brown BD, Sitia G, Annoni A, et al. In vivo administration of lentiviral vectors triggers a type I interferon response that restricts hepatocyte gene transfer and promotes vector clearance. *Blood.* 2007;109(7):2797-2805.

22. Onoe T, Ohdan H, Tokita D, et al. Liver sinusoidal endothelial cells tolerize T cells across MHC barriers in mice. *J Immunol.* 2005;175(1):139-146.

23. Jockusch H, Voigt S, Eberhard D. Localization of GFP in frozen sections from unfixed mouse tissues: immobilization of a highly soluble marker protein by formaldehyde vapor. *J Histochem Cytochem.* 2003;51(3):401-404.

24. Ganesan LP, Mohanty S, Kim J, Clark KR, Robinson JM, Anderson CL. Rapid and efficient clearance of blood-borne virus by liver sinusoidal endothelium. *PLoS Pathog.* 2011;7(9):e1002281.

25. Meurer SK, Tihaa L, Borkham-Kamphorst E, Weiskirchen R. Expression and functional analysis of endoglin in isolated liver cells and its involvement in fibrogenic Smad signalling. *Cell Signal.* 2011;23(4):683-699.

26. Kamentsky L, Jones TR, Fraser A, et al. Improved structure, function and compatibility for CellProfiler: modular high-throughput image analysis software. *Bioinformatics.* 2011;27(8): 1179-1180.

27. Seon BK, Matsuno F, Haruta Y, Kondo M, Barcos M. Long-lasting complete inhibition of human solid tumors in SCID mice by targeting endothelial cells of tumor vasculature with antihuman endoglin immunotoxin. *Clin Cancer Res.* 1997;3(7): 1031-1044.

28. Minhajat R, Mori D, Yamasaki F, Sugita Y, Satoh T, Tokunaga O. Organ-specific endoglin (CD105) expression in the angiogenesis of human cancers. *Pathol Int.* 2006;56(12):717-723.

29. Erslev AJ, Besarab A. Erythropoietin in the pathogenesis and treatment of the anemia of chronic renal failure. *Kidney Int.* 1997;51(3): 622-630.

30. VandenDriessche T, Thorrez L, Naldini L, et al. Lentiviral vectors containing the human immunodeficiency virus type-1 central polypurine tract can efficiently transduce nondividing hepatocytes and antigen-presenting cells in vivo. *Blood.* 2002;100(3):813-822.

31. Park F, Ohashi K, Chiu W, Naldini L, Kay MA. Efficient lentiviral transduction of liver requires cell cycling in vivo. *Nat Genet.* 2000;24(1):49-52.

32. Pfeifer A, Kessler T, Yang M, et al. Transduction of liver cells by lentiviral vectors: analysis in living animals by fluorescence imaging. *Mol Ther.* 2001; 3(3):319-322.

33. López-Novoa JM, Bernabeu C. The physiological role of endoglin in the cardiovascular system. *Am

J Physiol Heart Circ Physiol. 2010;299(4): H959-H974.

34. Mahmoud M, Borthwick GM, Hislop AA, Arthur HM. Endoglin and activin receptor-like-kinase 1 are co-expressed in the distal vessels of the lung: implications for two familial vascular dysplasias, HHT and PAH. *Lab Invest.* 2009; 89(1):15-25.

35. Friedman SL. Hepatic stellate cells: protean, multifunctional, and enigmatic cells of the liver. *Physiol Rev.* 2008;88(1):125-172.

36. Bredow S, Lewin M, Hofmann B, Marecos E, Weissleder R. Imaging of tumour neovasculature by targeting the TGF-beta binding receptor endoglin. *Eur J Cancer.* 2000;36(5):675-681.

37. Hong H, Yang K, Zhang Y, et al. In vivo targeting and imaging of tumor vasculature with radiolabeled, antibody-conjugated nanographene. *ACS Nano.* 2012;6(3):2361-2370.

38. Morizono K, Ku A, Xie Y, et al. Redirecting lentiviral vectors pseudotyped with Sindbis virus-derived envelope proteins to DC-SIGN by modification of N-linked glycans of envelope proteins. *J Virol.* 2010;84(14):6923-6934.

39. Morizono K, Xie Y, Helguera G, et al. A versatile targeting system with lentiviral vectors bearing the biotin-adaptor peptide. *J Gene Med.* 2009;11(8): 655-663.

40. Pariente N, Mao SH, Morizono K, Chen ISY. Efficient targeted transduction of primary human endothelial cells with dual-targeted lentiviral vectors. *J Gene Med.* 2008;10(3):242-248.

41. Work LM, Büning H, Hunt E, et al. Vascular bed-targeted in vivo gene delivery using tropism-modified adeno-associated viruses. *Mol Ther.* 2006;13(4):683-693.

42. Park F. Correction of bleeding diathesis without liver toxicity using arenaviral-pseudotyped HIV-1-based vectors in hemophilia A mice. *Hum Gene Ther.* 2003;14(15): 1489-1494.

43. Schurich A, Böttcher JP, Burgdorf S, et al. Distinct kinetics and dynamics of cross-presentation in liver sinusoidal endothelial cells compared to dendritic cells. *Hepatology.* 2009;50(3): 909-919.

44. von Oppen N, Schurich A, Hegenbarth S, et al. Systemic antigen cross-presented by liver sinusoidal endothelial cells induces liver-specific CD8 T-cell retention and tolerization. *Hepatology.* 2009;49(5):1664-1672.

45. Fonsatti E, Nicolay HJM, Altomonte M, Covre A, Maio M. Targeting cancer vasculature via endoglin/CD105: a novel antibody-based diagnostic and therapeutic strategy in solid tumours. *Cardiovasc Res.* 2010;86(1): 12-19.